KSME

Springer

Journal of Mechanical Science and Technology 35 (5) 2021

Original Article
DOI 10.1007/s12206-021-0401-y

Keywords:
· Convolution neural network
· Deep learning
· Damage identification
· Electromechanical impedance
· PZT sensor

Correspondence to:
Dansheng Wang
danshwang@hust.edu.cn

Citation:
Alazzawi, O., Wang, D. (2021). Deep convolution neural network for damage identifications based on time-domain PZT impedance technique. Journal of Mechanical Science and Technology 35 (5) (2021) 1809~1819.
http://doi.org/10.1007/s12206-021-0401-y

Received April 29th, 2020
Revised January 18th, 2021
Accepted February 1st, 2021

† Recommended by Editor
No-cheol Park

Deep convolution neural network for damage identifications based on time-domain PZT impedance technique

Osama Alazzawi[1,2] and Dansheng Wang[1]

[1]School of Civil and Hydraulic Engineering, Huazhong University of Sciences and Technology, Wuhan, China, [2]Department of Civil Engineering, College of Engineering, University of Wasit, Kut, Iraq

Abstract Recently, Intelligence-based structural health monitoring (SHM) methods have investigated widely. Most of these methods are for detecting and classifying different structural damages by the means of features extraction from the structural responses signals, for instance different back propagation artificial neural networks SHM based methods. However, automatic features extraction, that eliminates the need for expertise and performing visual inspection to evaluate structures status is still a big challenge. In this study, therefore, a novel convolution neural network-based algorithm along with a hybrid training method has been proposed to detect, quantify and localize structural damage. The proposed method has been evaluated experimentally, many damaged and undamaged structural conditions have been conducted, acquiring samples of time-domain PZT impedance response signals from a beam. As the results show that, the method obtained a significant execution on damage detection, damage size evaluation and damage location recognition with high accuracy and reliability.

1. Introduction

Civil infrastructures such as skyscraper, bridges, etc., are an essential part of the nation's economy due to their dominant role in facilitating the overall situation. Damages in any structural part may affect the structure functionality, leading economic and epidermal astronomical losses [1]. Structural health monitoring (SHM) is the main implemented tool for a damage identification strategy for any engineering structure [2]. To advance the prevention of any structural failure, many SHM methods have been applied to assess the conditions of the civil infrastructure. The structural dynamic analysis using mathematical or physical models has been widely used, however, a nonlinear has raised in most of the real-life implementations. This nonlinearity initiated by different factors such as, materials and geometries, etc., makes the used analytical model more complicated and overpriced. In this context, many researchers focused on the direct damage identification methods performed through the structural responses based on sensors networking [3-5].

Consequently, the impedance-based method is one of the promising NDE methods, based on lightweight, a low-cost and small piezoelectric transducer (lead zirconate titanate) bonded onto the critical parts of the structure. This method is widely discussed in the literature which is based on concept that a change in the mechanical properties will results in a variation in the PZT impedance signature [6-13]. Most of the impedance-based damage assessment developed approaches are observed to be a sort of feature extraction practice since they consider the variations among categories, e.g., the structural conditions before and after the structural damage have been accrued or variations in damage sizes. Deep learning was observed as a superior intelligence-based tool that has attracted several researchers for pattern recognition problems including the damage identification in civil structures.

Recently, wide investigations have been conducted to apply artificial neural networks in many SHM methods to assess the structural status. Different SHM approaches were introduced based on the backpropagation and multi-layer perceptron neural networks [14-16]. Subse-

quently, other sorts of ANN, for example, recurante neural network (RNN), fuzzy ARTMAP network (FAN), probabilistic neural network (PNN) are introduced. Many research successfully explored the methods of applications on several structures such as SHM methods are applied to damage detection and identification using PPN [17-19].

Similarly, one of the most important applications of deep learning in SHM methods is convolutional neural network (CNN) which has been investigated widely even in real-world applications. CNN is considered as one of the most advanced and effective deep learning models; it has also been applied in many areas such as face recognition, processing of natural language and engine fault detection [20-22]. The difference between CNN and the conventional ANN is the ability of CNN's layers to organize neurons in three dimensional (3D) way: height, width and length. Therefore, CNN is successfully utilized in numerous structural health monitoring areas based on accelerometer vibration signals. A fast and precise method was proposed for early fault detection system and motor condition monitoring by applying 1D-CNN [23]. The authors have followed the same approaches for the same purpose in Ref. [24]. Likewise, another method was introduced to address fault identification utilizing CNN on raw vibration signals without any preprocessing [25]. Similarly, in Ref. [26], a real-time damage detection and localization methods based on raw acceleration signals with 1D-CNN were proposed. Accordingly, in Ref. [27], they collected the raw training process data of CNN from multiple accelerometer sensors and analyzed the information temporally and spatially. In Ref. [28], the authors used a network and training process for each of the single assigned 1-D CNN for an individual wireless sensor in the sensors network using the locally-available data. Similar, in Ref. [29], an enhanced approach has been applied based on CNN that needs two measurement sets only irrespective of the structural size, their applied approach was capable of quantifying the existing damage quantity prosperously.

The CNN has been adopted for impedance-based structural damage detection of a plate with simple damage conditions [30]. However, limited studies based on purely deep CNN for impedance-based SHM applications, for example, damage identification on a more complex damage cases, has been conducted. Inspired by the above observations, a novel SHM framework is proposed based on deep CNN to achieve effective and efficient feature extraction of time-domain impedance signals that imitate the true structural damages. The proposed method was experimentally tested applying the PZT-EMI technique. The methodology was validated on a simply supported steel beam which is instrumented with five surfaces bonded PZTs transducers. The simulated damages were inserted into four scenarios, by creating small damage, moderate damage, severe damage and multiple damages at different positions. The PZT response signals were acquired in the time domain for all the mentioned scenarios and converted to time-frequency scalograms as RGB images and fed into hierarchically organized CNNs. As a results a superior accuracy was achieved through an accurate training regarding damage detection, quantification, and localization by applying the proposed method which operates on the PZT-EMI signals. The main contributions of this paper can be summarized as the following:

- A novel automated damage identification method was developed based on the time domain PZT-EMI response signals. A method that utilizes CNN for automatic features extraction from the PZT response signals of various structural conditions.
- The method organized in hierarchical architecture producing a two-layer of CNN algorithm, where the first layer is for damage detection and the second layer is for damage size and location evaluation.
- Unlike the other damage identification methods based on PZT-EMI signals showed in state of the art, the proposed methodology needs to operate the impedance time-domain signals eliminating the requirements of measuring the sensitive frequency domain signals within damage applied frequency range.
- A novel hybrid training method for the SHM algorithm, its decentralized from a side enabling each of the CNNs to detect damage at the corresponding PZT regardless the rest of CNNs, and centralized from another side combining in a single class all of the signals that measured at different damage conditions (damage classes).
- The EMI technique weakness of low sensitivity to incremental and multiple damages was utilized as an advantage by combining all the PZT response signals throughout the different damage conditions resulting in a system capable of detecting structural damages with several sizes and locations directly.
- A new damage size estimation method was proposed, which is based on the soft-max classification layer.
- Damage localization has been achieved using RMSD in a new application which is different in the purpose from its conventional application for damages quantification.

In the meantime, the impedance-based structural health monitoring and convolution neural work are described in Sec. 2, followed by the explanation of the proposed methodological for structural damage detection, quantification and localization and EMI time-domain acquisition system and the conversion method of the signals to RGB images in Sec. 3. In Sec. 4, description of the experimental work. Finally, the presentation of the experimental results obtained in this study are described in in Sec. 5 and compared with other method in Sec. 6, and the conclusions in Sec. 7.

2. Related works

This section presents the associated works including electromechanical impedance (EMI) technique for structural health monitoring (SHM) and the convolution neural network (CNN).

2.1 The electromechanical impedance (EMI) technique for structural health monitoring

The electromechanical impedance (EMI) technique utilizes a surface bonded or embedded low-cost piezoelectric transducer (PZT) on or in critical structural parts of the monitored structure. The PZT is capable to produce excitation on the host structure with a wide range of applied frequency and acquires the excitation response of the host structure. Therefore, EMI technique possess a significant position in the field of SHM [30].

The basic concept of the mentioned technique is based on measuring the PZT transducer electrical parameters after attaching it to the host structure. An electromechanical response is conceived due to the interaction of the piezoelectric transducer and the monitored structure, where the electrical characteristics of the PZT transducer are affected by the mechanical response of the structure. PZT transducer covers a wide frequency range (from a few Hz up to GHz) with an effective electromechanical interaction, suitable stability, high response to electric excitation and stiff [30]. The EMI technique has high sensitivity to detect early-stage damages, but its actions are limited spatially. The EMI method has been applied in various SHM systems, including civil structures, industrial machines, airplanes, mechanical tools and processes of machining [31-33].

The first one-dimensional equation that formulates the electrical and mechanical impedance relationship was proposed by Liang [34]:

$$Y(\omega) = i\omega a[\varepsilon^T(1-\iota\delta) - \frac{Z_s(\omega)}{Z_s(\omega)+Z_A(\omega)} d_{3x}^2 Y^E \quad (1)$$

where $Y(\omega)$ is the electrical admittance of the PZT element. $Z_S(\omega)$ And $Z_A(\omega)$ are the mechanical impedance of the host structure and PZT, respectively. By observing the electrical admittance, any changes in this impedance can be detected. a, ε^T, d_{3x}^2, Y^E are the constant of transducer geometric, zero stress dielectric constant, dielectric loss tangent, piezoelectric coupling constant and complex Young's modulus of the transducer at the zero electric fields, respectively. In the EMI method observation and analytical process for electrical parameters such as impedance with both of its real and imaginary parts (resistance, reactance) in addition to the admittance also with its real and imaginary parts (conductance, susceptance) are conducted. The stat of art shows that the attachment layer between PZT transducer and host structure can be assessed using imaginary part of electrical parameters to monitor the PZT transducer [35], whereas the real part of electrical parameters is used for monitoring of the under-assessment structure.

2.2 Structural damage detection based on time domain impedance

By the comparison of the time domain analysis methods and the frequency-domain analysis of the EMI technique, it is clear that the former is reasonable for structural damages detection. Similarly, there is a limited literature on this topic. The damage detection can be achieved efficiently by using the time-domain method. Inman et al. [35] have successfully detected damages by utilizing the wavelet transform through the comparison of correlation coefficient deviation metric (CCDM) and root mean square deviation (RMSD) indexes of the EMI response in frequency-domain. For the time-domain analysis a circuit of excitation on the PZT and host structure is needed, as shown in Fig. 1.

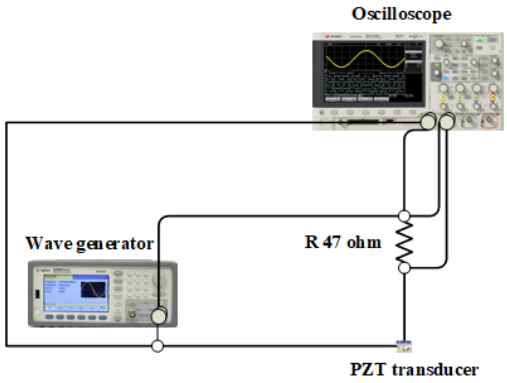

Fig. 1. Electromechanical impedance measurement system for time-domain signals.

Mostly in time domain-based damage detection, a comparison is conducted in between the electrical voltage changes in the PZT transducers response signals and PZT transducer surface bonded/embedded on or in the host structure.

2.3 The propose and background of CNN

CNN has been successfully applied in automatic feature extraction, evidencing its fully supervised learning and standardized gradient descent. In general, the CNN model composed of two parts one for feature extraction and other multi-layer perception for classification.

A convolution layer and a max-pooling layer forming the feature extraction part. The features of the RGB images are extracted by the convolution layer, the main function of the max-pooling layer decreases the consumed time of processing and increases the invariability between structure and space progressively, meanwhile the main properties of the RGB images maintained. Accordingly, a multi-layer perceptron classifier's input is the extracted features. Hidden layers and output layers are the basic structure of the multi-layer perceptron classifier; Fig. 2 shows the typical CNN structure. All of the CNN's nodes having the same activation function, the most popular activation function is so-called a sigmoid function. The automatic feature extraction theoretical concept using the CNN method is explained in secstions 2.3.1 and 2.3.2.

The authors designed a hierarchical CNN model for feature extraction and used a hybrid training method for damage de-

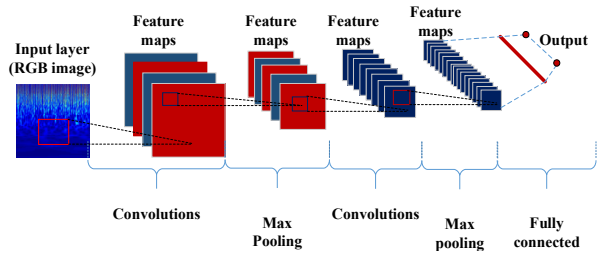

Fig. 2. Typical convolution neural network (CNN).

tection and quantification phases from the PZT transducer response signals. In addition, as shown in Fig. 3, a compressed CNN model is implemented to reduce the time consummation and increase the procedure simplicity. Therefore, each CNN model is built with image input layer, two convolution layers, two max-pool layers, fully-connected layers, softmax layer, and classification output layer.

2.3.1 Feed-forward operation

Referring to the time domain PZT transducer signals samples $\{X,Y\}$ assume X and Y are the input signals vectors and the target classes, respectively, called the structural conditions. The number of data-set samples is N. It is possible to transform the input signal into an RGB image with various dimensions. The convolution layer as per its functionality generates new maps of features called features maps, the kernels (filters) is convolve the features maps in the mentioned layer [36]. Convolution of several input features resulting in the output map. The definition of feature maps progress in a convolution layer is:

$$O_j^l = f(\sum_{i\in Mj} \sigma_{ij} O_i^{l-1} * w_{ij}^l + b_j^l) \tag{2}$$

where O_i^{l-1} is the output of the $l-1$ th layer and w_{ij}^l the input into the next layer through the feature map i, and o_j^l is the jth feature map of the $l-1$ *th* layer. $f(o)$ for the sigmoid function, M_j is a selection of input maps and is the kernel weight linking the i th feature map of the $l-1$ th layer with the jth feature map of the $*$ th layer $*$ denotes the process of convolution. An additive bias b, is given to each output map. Through several kernels, the input feature maps related to a specific out-put feature map are convolved. Within the convolution operation, every out-put feature map has the same weight distribution and size, for *s* reduction of the training parameters. The following formula used is for producing the features maps of the sub-sampling layers:

$$O_j^l = f(\delta_j^l S(o_j^{l-1} + b_j^l)) \tag{3}$$

where $S(o)$ is the function maximizes every class with a specific size in the feature map which is named as max pooling, and δ_j^l is the deviation in the multiplier for the jth feature map of the l th layer. The important advantage of CNN is the

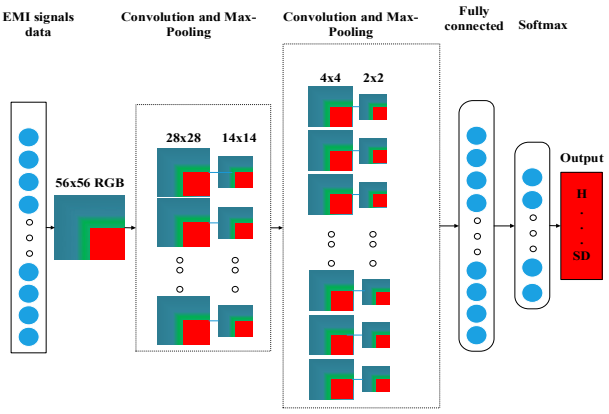

Fig. 3. The proposed configuration for the convolution neural network (CNN).

ability to extract features automatically through its layers one by one. Every layer of CNN is considered as a feature map for the next layer. The feature extractors are weights and bias linking two of layers. The spatial property of the last feature lays in the neurons' number of CNN's final layers. The weights and bias for all of the layers are updated using gradient descent to achieve the highest performance accuracy.

2.3.2 Back propagation and gradient descent

Back-propagation is used to compute the loss function gradient for all layers and weights. The objective function is specified using a function of squared error loss. The problem is multi-class with m several classes and N data-set samples. As an explanation, after training one sample the function of loss is presented in Eq. (4), n is the calculated loss function overall, as follows:

$$E^n = \frac{1}{2}\sum_{k=1}^{m}(l_k^n - y_k^n)^2 \tag{4}$$

where the training sample index is n, and the label index is *k*. Here, in a sample n the corresponding k th label is l_k^n and the output-layer unit value is y_k^n. In problems of classification of multiclass, a vector presents the out-put mostly, the positive is the class out-put node related to the dimension of the input only. The remaining nodes of the class are negative or zero, depending on the output layers activation function, where the *tanh* function is 1 and the sigmoid function is 0. Subsequently, in a layer from neurons u to neurons v the sensitivity of neuron φ_j^l is computed, and the function of loss gradient for the kernel weights is calculated by back-propagation as follows:

$$grd = \frac{\partial E}{\partial W_{ij}^l} = \sum(\varphi_j^l)_{u,v}(O_j^{l-1} W_{ij}^l)\,. \tag{5}$$

2.4 The continuous wavelet transform (CWT)

The continuous wavelet transform (CWT) is one of the most

important tools in signal processing, due to the fundamental collaboration between physics and signal processing known by Gabor, Morlet, and Grossmann, has led up to the formulation of the (CWT) [37]. Continuous wavelet transformer promotes the continues variation of the wavelets scale parameter and translation producing a professional representation of a signal. Based on a mother wavelet ψ of zero average a wavelet dictionary has been constructed

$$\int_{-\infty}^{+\infty} \psi(t)dt = 0\,, \tag{6}$$

which is translated by u, with a scale parameter s dilation:

$$D = \{\psi_{u,s}(t) = \frac{1}{\sqrt{s}}\psi(\frac{t-u}{s})\}_{u\in R,\, s>o}\,. \tag{7}$$

At any scale s, and position u the continues wavelet transform of f is equal to the projection of f on the wavelet corresponding atom:

$$Wf(u,s) = \langle f, \psi_{u,s}\rangle = \int_{-\infty}^{+\infty} f(t)\frac{1}{\sqrt{s}}\psi^*(\frac{t-u}{s})dt\,. \tag{8}$$

It is a one-dimensional representation of signal by lengthy timescale images in (u, s).

3. The proposed damage identifications method

As mentioned earlier, four structural damages are experimentally simulated in a simple supported beam, the created damages are small damage, moderate damage, severe damage and multiple damages for different positions consequently. The proposed EMI-CNN algorithm is aiming to detect the damage in case of incidence, quantify the size of the damage and identify the locations of the damages accurately. The implementation of the EMI-CNN algorithm needs constructing and training a single assigned CNN for each one of the five PZT transducers. The responsibility of all of the five CNNs is condition assessment of the beam using time-domain PZT transducer response signals measured at the beam. Firstly, each of the five CNN (CNN 1, CNN 2, CNN 3, CNN 4, and CNN 5) has trained to classify into two structural conditions, one is healthy condition while the second condition is damages in all sizes and locations (the four simulated damage).

It is considered a single condition by combining the measures of PZT signals under one class to increase the accuracy and centralize the method. Once the signal classified as damage condition class then the testing signals of the first fourth CNNs fed to another four CNN of PZT1 to quantify and locate the damage (CNN 1-1, CNN 1-2, and CNN 1-3 for damage severity evaluation) the (CNN 1-4 for damage localization). So on for all the PZTs, irrespective of the methodology and hierarchical architecture. Therefore, the EMI-CNN algorithm enabled each CNN to detect damages at its PZT separately from the other CNNs. The proposed damage detection algorithm decentralized from a side and centralized from another side which makes it a hybrid method.

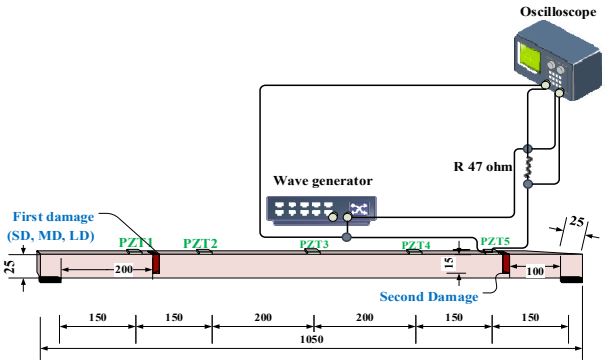

Fig. 4. Illustration of the general diagram of the signals acquisition method (dimensions in millimeter).

3.1 Damage size quantification

Next, to the damage detection, four CNNs are implemented for each PZT. These four CNNs have constructed with architecture similar to that of CNN in the damage detection layer, due to the similarity of sample dimensions. While, the test RGB images forms the input of the mentioned layer after training, and a class label along with the probability vector as an output, specifying the used sample affiliated to each class and the probability of the affiliation simultaneously. A sample label was proposed because of the importance of size identification, a method of the damage size estimation of each sample. The labels of classes are noted as 1, 2, ..., N for a case has N classes, the soft-max method is utilized for calculating the probability of each sample class and size affiliation as follows:

$$Po(x_i) = \{Po_1, Po_2, ... Po_N\}\,. \tag{9}$$

Consequently, the depth of damage is calculated as follows:

A probability threshold value has set to be 95 %, in other words only the sample classified with higher than 95 % probability of belonging to jth class has been considered. Mean of probabilities that equal or higher than the set threshold value calculated as:

$$MeanPo_j = \frac{\sum P_{o\geq 95\,\%}}{N}\,. \tag{10}$$

While the size of the damage is calculated as:

$$SoD = (D_j \times MeanPo_j) \mp 0.01 \tag{11}$$

where D_j is the specified size of damage for the jth damage class. $MeanPo_j$ is the affiliation probability of the *N* samples to the jth damage class. ∓ 0.01 is a correction factor which is equal to the loss value.

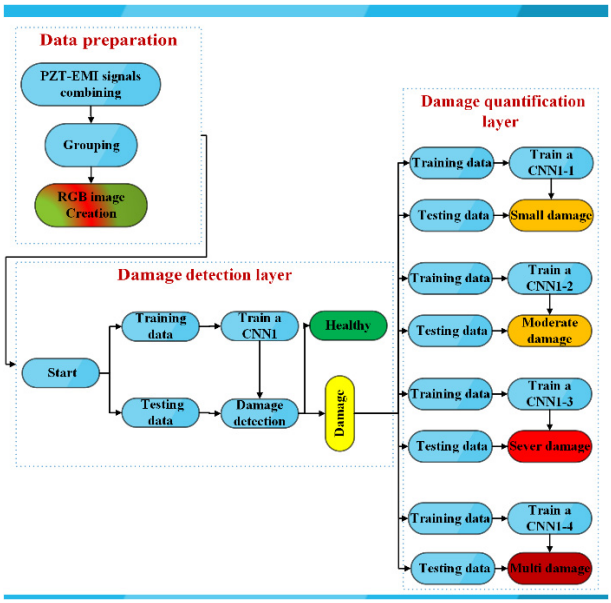

Fig. 5. Scheme of the data perpetration and the architectural hierarchy of CNN.

3.2 Damage localization using root mean square deviation

Usually, damage index is important for condition assessment of structures which depends on the real part of the PZT sensor's impedance as indicator of condition changes, through observing the changes and quantify the damage statistically. The mean function is a helpful tool to arrange and analyze big data set. When the variations of the quantities are positive and negative for example sinusoidal wave, root means square (RMS) is a power-full statistical measure to obtain the number of variations. For different signals, RMS value can be considered as samples of equal space. The sum of samples divided by the number of these observations (N) resulting in the average (mean). The reality of damage and the voltage deviation can be measured by applying the root mean square. Mostly, RMSD as a statistical measure was used for damage quantification [8-13]. In this work, root mean square is adapted to locate the damage by measuring the changes in voltage at each PZT with its respective location on the beam and generating an illustration similar to the damage map, for each damage location and size. Following equation defines the RMSD,

$$RMSD\% = \sqrt{\frac{\sum_{i=1}^{N}(Z_{1,i} - Z_{2,i})^2}{\sum_{i=1}^{N} Z_{1,i}^2}} * 100 \quad (12)$$

where Z_1 and Z_2 are the reference for the measured signals and the measured signal used for comparison, respectively, i is the measurement interval and N is the total number of samples used for comparison [5].

Table. 1. Experimental damage description.

Structural condition	Crack depth	Location
Healthy	-	-
Small damage (SD)	5 mm	200 mm to the left support
Moderate damage (MD)	10 mm	200 mm to the left support
Severe damage (LD)	15 mm	200 mm to the left support
Multiple damage (multiD)	15 mm	100 mm to the right support

4. Experimental work

We established a method based on the PZT-EMI method for obtaining the PZT-EMI response signals in time-domain, which considers the response signals of the structure. EMI is applied by exciting the monitored structure using a PZT at a frequency of wide range and of low amplitude to create an excitation force on the monitored structure [6]. Generally, PZT can act as a sensor or actuator, EMI technique uses the PZT transducer as actuator and sensor at the same time. In our case, a steel beam of 1050 mm length, 25 mm width and 25 mm depth was simply supported. Five piezoelectric patches (PZT 1, PZT 2, PZT 3, PZT 4, and PZT 5) with the size of 10 mm× 10 mm×1 mm were utilized, that had active elements of type P-7 PZT ceramics. PZT was attached on the upper surface of the beam at five selected positions as shown in Fig. 6, where the bonding material used is 3M Scotch-Weld Epoxy Adhesives DP460 Off-White. Subsequently, a frequency-range of 0-500 kHz with an amplitude of 1 V was used to initiate the excitation on the PZT and structure. The properties such as mass, shape, boundary condition, and other structural properties all effect and control the sensitivity of the EMI signals frequency band [7]. Similarly, researches revealed that the high frequencies decrease interactions of global properties in the vibration modes of structure [12], which maintain the selected range of frequency.

The electro-mechanical impedance measurement system was utilized to produce excitation and acquire the responses of the structure. As shown in Fig. 2 the electric current passing through the PZT patch was controlled using 47 Ω resistor (R). Various structural conditions are implemented, and measurements using the mentioned system were conducted. Firstly, the measured signals were saved to create a healthy condition. Each PZT measure was sampled independently at a sampling rate of 5000 sample/second. Next, four damage cases were simulated consequently by creating small damage, moderate damage, severe damage and multiple damages for two different positions in the structure (Figs. 4 and 6). The size of the damage increased gradually started with 5 mm for small, damage 10 mm for moderate damage and 15 mm for severe damage as depth, the first three damage cases (named SD, MD, and LD) and in the fourth damage case is a new damage of 15 mm depth in a different location was created in addition to the 15 mm crack at 200 mm from the left support (named multiD) as portrayed in Table 1.

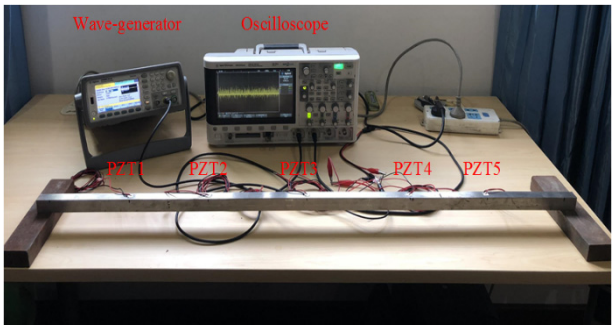

Fig. 6. Setup of experiment composed of: steel beam instrumented with five PZT patches, arbitrary waveform generator, a reference resistor, and oscilloscope.

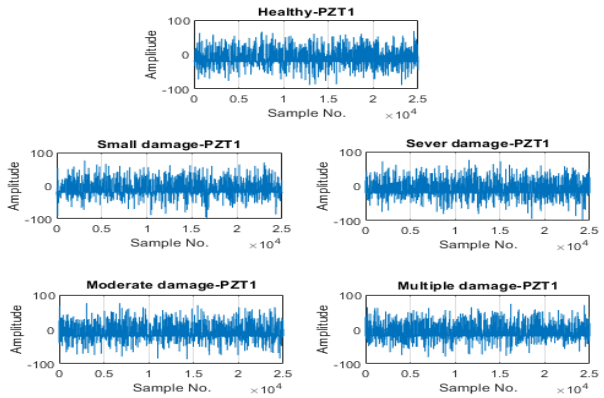

Fig. 7. Sample PZT signals from the healthy and damaged beam.

Hence considering SD, the PZT 1 was excited separately, and its related signal is acquired on an individual basis, followed by all the PZTs with the same procedure. Following this method, the measures are obtained individually for each patch of the five PZT transducer, by promoting the approach to perform on any response signals independently. Then, the damage depth increased to 10 mm MD. Again, the response signals for PZT 1, PZT 2, PZT 3, PZT 4, and PZT 5 were acquired individually. Finally, the same approach was repeated for LD and multiD. In total, there were 2500 time-domain PZT-EMI signals (500 for each structural condition/ five PZTs). The response signals were obtained for 500 seconds from each PZT in the respective structural condition. The used sampling rate was 5000 sample/second with the signal length 25000 sample. Thereby, conducting the measurements 100 times for every PZT at each structural condition resulting in acquired PZT response signals for about eight minutes. Meanwhile the room temperature was maintained at 27 °C during the experiment. RGB images were formed using PZT-EMI response signals.

4.1 The continues wavelet transformer (CWT) for the PZT time-domain signals to RGB (red, green, and blue) images scale

The state of art SHM approved that there are some rare applications of CNN as an automatic feature extractor along with PZT-EMI based structural health monitoring method due to the complexity of converting the PZT transducer responses signal to meaning-full images or videos form. While addressing this issue, we proposed an effective way to form scalograms (RGB images) from time domain PZT-EMI signatures by utilizing CWT function filter bank in (MATLAB). The procedure to produce RGB images is as follows:

1) Loading all the raw EMI data into a matrix containing all the sampled measurements;

2) All the EMI data stored in structure including an array (double) for data (sampled signals) and cell for the training labels as (healthy and damage) conditions;

3) The EMI signals for (healthy (H) and small damage (SD)) conditions are grouped in new structure containing a matrix for the sampled signals for the mentioned conditions and cell for the training labels;

4) The same procedure in Eq. (3) was repeated for three times to prepare the data for the rest of the structural conditions;

5) Using continuous wavelet transform filter bank function (MATLAB), all the EMI data and the grouped data are converted to scalograms as 56x56 RGB images;

6) Each measured PZT response signals was converted to single 56x56 RGB image;

7) The created images are then stored as a JPEG image in pre-made directories named as same to the label names. The input of CNN is the images by feeding them through the CNN input layer.

5. Experimental results

In the evaluation of the developed approach, this section headlines the results acquired by implementing the experimental set up. Firstly, the signals of the structural response were acquired through the PZTs from the different structural conditions, using the measurement system discussed above. Sample signals are shown in Fig. 7 where the time-domain impedance for PZT 1 is presented. Signatures are presented for five various kinds of structural conditions: healthy (H), small damage (SD), moderate damage (MD), severe damage (LD), and multi-damage (multiD).

As determined, the damage incidence will produce a difference in the PZT-EMI response signals due to the variations in the PZT electro-mechanical impedance. At various structural conditions, the incremental accumulative and multiple structural damages produce only incipient changes in the EMI signatures which need an accurate method for the detection of variations in automatic signals.

Secondly, the acquired signals of the structural response were grouped and converted to RGB images applying the continuous wavelet transform. Fig. 8 illustrates a set of the RGB images produced by converting the EMI signatures for PZT1 using the continuous wavelet transformer. The images shown in Fig. 8 are produced for signatures of the healthy (H) and all

Table. 2. The RGB images formed from each PZT transducer response signal.

No.	Structural condition	Training samples	Test samples
1	Healthy (baseline)	70	30
2	Small damage (SD)	70	30
3	Moderate damage (MD)	70	30
4	Multi-damage (multiD)	70	30

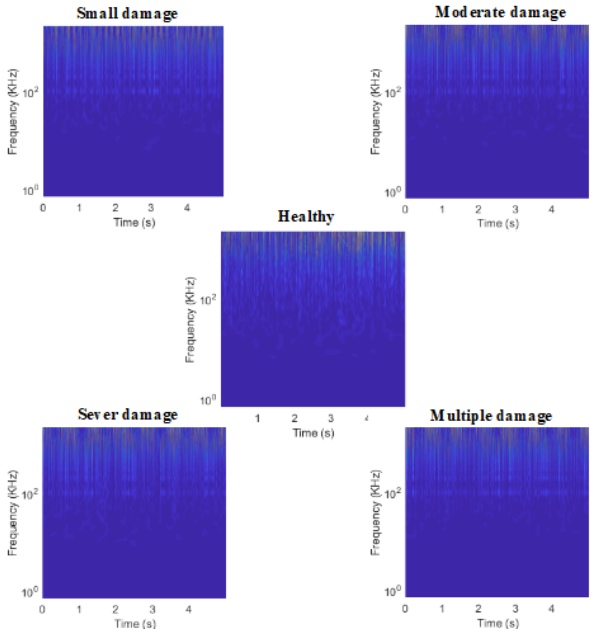

Fig. 8. The created RGBs using CWT for all of the structural conditions (healthy, SD, MD, LD and multiD).

of the damaged structural statuses, respectively. A perceptible variation is shown between healthy and damage structural conditions through the RGB in Fig. 8. Meanwhile there are imperceptible changes which couldn't be observed by naked eye, which demonstrate that we have conducted subtle analysis on the images. Contrarily, if we consider various structural damage conditions RGBs, then such variations are hard to inspect and need algorithm with a high-efficiency training method to overcome.

Accordingly, this method uses a hybridized training method and utilizes the hierarchical architectural arrangement for the CNN algorithm to get the benefit of those small variations to achieve accuracy and reliability in the damage detection method. It is necessary to mention that the created RGB images are used to make an image data store for training, evaluation, and testing of the CNNs, which formed the input to the CNN algorithm Table 2.

In the same way, the dataset (image data store) is fed to the proposed CNN model. The CNN trained and tested on a Laptop has an Intel C i5-2450 M, 4 GB of RAM and running Windows 7. The training and testing conducted on the mentioned

Fig. 9. First convolutional layer weights.

laptop CPU without GPU.

The well-known MATLAB software was used to write and run the systematic program of the proposed approach. The CNN parameters were set by the trial and error method. The size of the batch and the number of the epoch were set to 8 and 20 consequentially. It has been observed from the earlier epoch during the training process coverage. Five CNN models were designed to detect any kind of damage, one CNN assigned for each PZT sensor in the first layer (damage detection layer) of the model. In the second layer (damage quantification and localization layer) of the mentioned model, another four CNN was implemented for each PZT sensor, each of them responsible for detecting one of the simulated damage cases. Resulting in a CNN model able to detect any type of damage, quantify and localize the later.

CNN model composed of some layers in general, where each layer produces an activation on the input image. The first layer of the network captures the basic features of an image such as edges. Fig. 9 shows the first convolution layer weights after applying 6 kernels onto a certain RGB for PZT 1. As shown in Fig. 10, if we compare the healthy (H) and combined damaged structural conditions, there are significant variations among the feature maps of the healthy and combined structural damaged states. These variations are a positive indication of the fittings of the introduced method.

Similarly, for the CNNs in the quantification layer (CNN 1-1, CNN 1-2, CNN 1-3, and CNN 1-4). Each one of the mentioned CNNs assigned to classify into two structural statuses, healthy and one of the simulated damages starting with SD. After applying six kernels to PZT 3 RGB images considering H, SD, MD, LD, and multiD structural conditions. Analyzing the results shown in Fig. 11 it is clear to perceive how PZT 3 recognizes each structural situation. Also, for each RGB image, it is evident that it is considered as a promising identifiable feature by comparing with RGB shown in Fig. 8 for each structural condition, thus, awarding this method a precise outstanding application in SHM.

After the training and testing processes for each of the CNNs, these are already designed for each PZT transducer; CNN is observed to be fitted after almost two epochs. All CNNs results for each PZT shown in Table 3. These results show clearly that the high efficiency of the current approach is with 100 % accu-

Table 3. The results of damage detection and size evaluation.

Healthy (baseline)	Training accuracy %	Test accuracy %
Small damage (SD)	100	100
Moderate damage (MD)	100	100
Sever damage (LD)	100	100
Multi-damage (multiD)	100	100

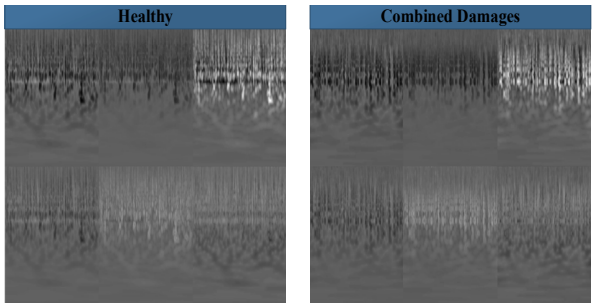

Fig. 10. Extracted features from PZT RGB images through the second convolution layer.

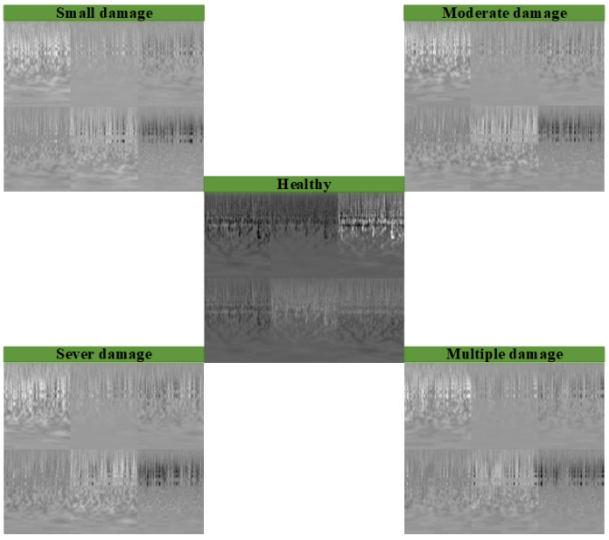

Fig. 11. Extracted features from PZT 3 RGB images of each structural condition.

racy, revealing that the proposed methodology is capable of detecting and quantifying different structural damages conditions. These results were achieved with a simple training set for the CNN without any GPU Table 1. It is considered a superior and precise solution for practical applications since it depends on the training data-set from available measured signals which represents the response of the structure.

In order to locate the damages by quantifying the change in the measured voltage due to damages, the RMSD index is utilized. All calculations in this work have been derived from the measured time domain voltage. The RMSD percentage was increased as the crack depth increased. The final comparison of RMSD percentage between collected healthy and different damages from several PZTs results evidenced that with increase in the damage size and number, the RMSD of the near to damage PZT transducer is also increased. RMSD values of PZT 5 and PZT 4 were increased significantly when the first damage was applied. Similarly, when the second damage created the RMSD value of PZT 1 also increased indicating that damage has occurred nearby its location. It is concluded from these results that the RMSD can be used to locate the damage which reveals its another essential application for damage localization along with damage quantification Fig. 12.

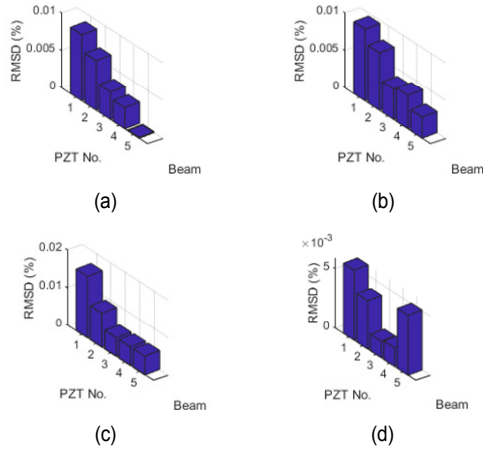

Fig. 12. RMSD for localization of different damages: (a) small damage; (b) moderate damage; (c) sever damage; (d) multi-damage.

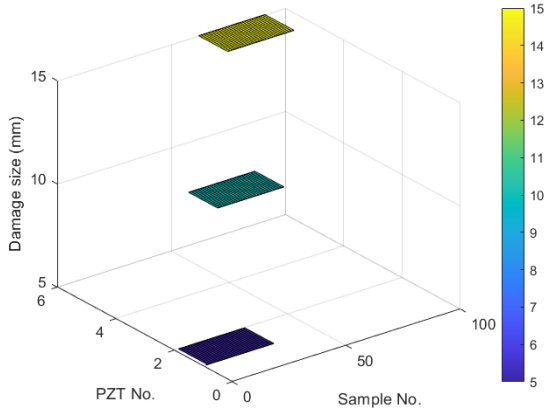

Fig. 13. Testing results of the damage size evaluation.

6. Comparison of the proposed damage quantification method with RMSD

The proposed method for damage size quantification provides an accurate method of diagnosing damage size which demonstrated an efficient way to figure out the issue of damage size evaluation. The performance of the proposed method compared to the existing typical RMSD method, to sustain its superiority. Fig. 13 illustrates the damage size evaluation achieved by the proposed damage quantification method for all of the damage sizes (5 mm, 10 mm, 15 mm) using the twenty testing samples for each PZT. Similarly, Fig. 14 shows the

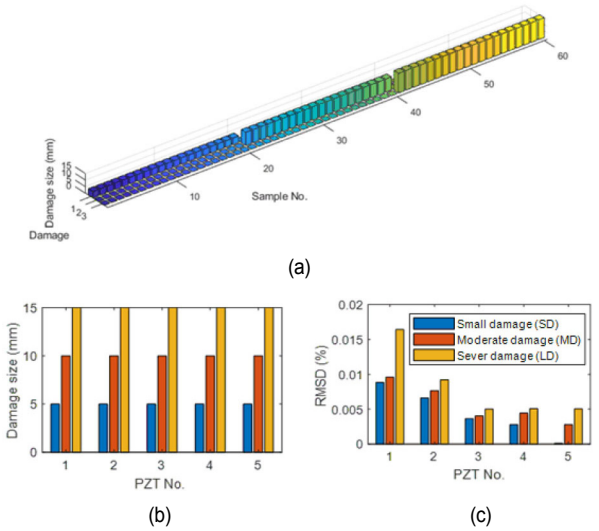

Fig. 14. Damage size quantification of the testing samples for each damage size: (a) and (b) proposed method; (c) RMSD.

comparison of the damage size evaluation achieved by the newly proposed method and the RMSD. The second layer of the proposed two-layer CNN model performs better than the RMSD method.

The proposed method offers a more accurate tool of damage quantification through automatic extraction features, particularly when structural steel members are involved as compared to the damage quantification method of RMSD, which is significantly limited. The obtained results efficiently sustain the applicability of the proposed CNN model.

7. Conclusions

In this work, a novel CNN based model is proposed, and the utilization of this model to damage detection, damage quantification, and damage location evaluation is addressed. First, an effective centralized and decentralized training method is introduced, obtaining a CNNs capable to extract features from time-domain PZT signals automatically. Second, a hierarchical arrangement is implemented and the method is organized hierarchically to form a CNN model of two-layer. The damage detection is achieved in the first layer and the damage size and location assessment regarding three damage size conditions in two locations have been done in the second layer. Third, training and testing samples from a damage detection data-set are used to train and test the CNN models, for the mentioned experimental purposes samples data-set are collected. Moreover, the proposed approach was implemented in CPU using a simple training dataset while neglecting the need for a GPU. Fourth, in addition to an accurate damage detection method, an efficient damage size quantification method has been proposed, which makes a new use for the CNN's output. Fifth, a new damage localization method has been developed through calculating RMSD for each PZT for the different structural conditions. The results demonstrate that we have achieved a huge success for SHM using the hybrid CNN's training method along with the hierarchical CNN model. Based on our results, the EMI-CNN algorithm for SHM with a hit rate of 100 % was developed which represents a robust and reliable structural damage identification methodology.

Acknowledgments

The authors acknowledge the supports of the National Natural Science Fund of China (51278215) and Basic Research Program of China (contract number: 2016YFC0802002). The authors also gratefully acknowledge the work of the reviewers.

References

[1] X. M. Zhao et al., Vibration-based fault diagnosis of slurry pump impellers using neighbourhood rough set models, *Proc. Inst. Mech. Eng. Part C: J. Mech. Eng. Sci.,* 224 (4) (2010) 995-1006.

[2] C. Stolz and M. Neumair, Structural health monitoring, in-service experience, benefit and way ahead, *Struct. Heal. Monit. An Int. J.,* 9 (3) (2010) 209-217.

[3] S. J. S. Hakim and H. A. Razak, Modal parameters based structural damage detection using artificial neural networks - a review, *Smart Struct. Syst.*, 14 (2) (2014) 159-189.

[4] M. R. Hoseini, X. Wang and M. J. Zuo, Estimating ultrasonic time of flight using an envelope and quasi maximum likelihood method for damage detection and assessment, *Measurement,* 45 (2012) 2072-2080.

[5] S. J. S. Hakim, H. A. Razak, S. A. Ravanfar and M. Mohammadhassani, Structural damage detection using soft computing method, *Struct. Health Monit.*, 5 (2014) 143-151.

[6] P. Zhou, D. Wang and H. Zhu, A novel damage indicator based on the electromechanical impedance principle for structural damage identification, *Sensors (Basel)*, 18 (7) (2018) 2199.

[7] G. Park, H. H. Cudney and D. J. Inman, An integrated health monitoring technique using structural impedance sensors, *J. Intell. Mater. Syst. Struct.*, 11 (6) (2000) 448-455.

[8] G. Park et al., Overview of piezoelectric impedance-based health monitoring and path forward, *Shock Vib. Dig.*, 35 (6) (2003) 451-463.

[9] P. Selva et al., Smart monitoring of aeronautical composites plates based on electromechanical impedance measurements and artificial neural networks, *Eng. Struct.*, 56 (2013) 794-804.

[10] F. G. Baptista and J. V. Filho, A new impedance measurement system for PZT-based structural health monitoring, *IEEE Trans. Instrum. Meas.*, 58 (10) (2009) 3602-3608.

[11] S. Na and H. K. Lee, Resonant frequency range utilized electro-mechanical impedance method for damage detection performance enhancement on composite structures, *Compos. Struct.*, 94 (8) (2012) 2383-2389.

[12] M. A. de Oliveira et al., A new approach for structural damage detection exploring the singular spectrum analysis, *J. Intell. Mater. Syst. Struct.*, 28 (9) (2017) 1160-1174.

[13] V. Mallardo and M. H. Aliabadi, Optimal sensor placement for structural, damage and impact identification: a review, *SDHM Struct. Durab. Heal. Monit.*, 9 (4) (2014) 287–323.
[14] V. Lopes et al., Impedance-based structural health monitoring with artificial neural networks, *J. Intell. Mater. Syst. Struct.*, 11 (3) (2000) 206-214.
[15] A. Saxena and A. Saad, Evolving an artificial neural network classifier for condition monitoring of rotating mechanical systems, *Appl. Soft Comput. J.*, 7 (1) (2007) 441-454.
[16] E. Papatheou et al., A performance monitoring approach for the novel lillgrund offshore wind farm, *IEEE Trans. Ind. Electron.*, 62 (10) (2015) 6636-6644.
[17] S. Na and H. K. Lee, Neural network approach for damaged area location prediction of a composite plate using electromechanical impedance technique, *Compos. Sci. Technol.*, 88 (2013) 62-68.
[18] V. Mallardo, Z. Sharif Khodaei and F. Aliabadi, A Bayesian approach for sensor optimisation in impact identification, *Materials (Basel)*, 9 (11) (2016) 946.
[19] F. Al Thobiani et al., An application to transient current signal based induction motor fault diagnosis of Fourier-Bessel expansion and simplified fuzzy ARTMAP, *Expert Syst. Appl.*, 40 (13) (2013) 5372-5384.
[20] A. H. Aljemely, J. Xuan, F. K. J. Jawad, O. Al-Azzawi and A. S. Alhumaima, A novel unsupervised learning method for intelligent fault diagnosis of rolling element bearings based on deep functional autoencoder, *Journal of Mechanical Science and Technology*, 34 (11) (2020) 4367-4381.
[21] M.-K. Shin, W. J. Jo, H. M. Cha and S.-H. Lee, A study on the condition based maintenance evaluation system of smart plant device using convolutional neural network, *Journal of Mechanical Science and Technology*, 34 (6) (2020) 2507-2514.
[22] S.-Y. Lee and S.-K. Lee, Deep convolutional neural network with new training method and transfer learning for structural fault classification of vehicle instrument panel structure, *Journal of Mechanical Science and Technology*, 34 (11) (2020) 4489-4498.
[23] X. Guo, L. Chen and C. Shen, Hierarchical adaptive deep convolution neural network and its application to bearing fault diagnosis, *Meas. J. Int. Meas. Confed.*, 93 (2016) 490-502.
[24] Z. Tang et al., Convolutional neural network-based data anomaly detection method using multiple information for structural health monitoring, *Struct. Control Heal. Monit.*, 26 (1) (2019) e2296.
[25] R. Zhao et al., Deep learning and its applications to machine health monitoring, *Mech. Syst. Signal Process.*, 115 (2019) 213-237.
[26] O. Abdeljaber et al., Real-time vibration-based structural damage detection using one-dimensional convolutional neural networks, *J. Sound Vib.*, 388 (2017) 154-170.
[27] M. Xia et al., Fault diagnosis for rotating machinery using multiple sensors and convolutional neural networks, *IEEE/ASME Trans. Mechatronics*, 23 (1) (2018) 101-110.
[28] O. Avci et al., Wireless and real-time structural damage detection: a novel decentralized method for wireless sensor networks, *J. Sound Vib.*, 424 (2018) 158-172.
[29] O. Abdeljaber et al., 1-D CNNs for structural damage detection: verification on a structural health monitoring benchmark data, *Neurocomputing*, 275 (2018) 1308-1317.
[30] M. A. de Oliveira, A. V. Monteiro and J. V. Filho, A new structural health monitoring strategy based on PZT sensors and convolutional neural network, *Sensors (Switzerland),* 18 (9) (2018) 2955.
[31] F. Jia et al., Deep neural networks: a promising tool for fault characteristic mining and intelligent diagnosis of rotating machinery with massive data, *Mech. Syst. Signal Process.*, 72-73 (2016) 303-315.
[32] S. Park, C.-B. Yun and D. Inman, Structural health monitoring using electro-mechanical impedance sensors, *Fatigue Fract. Eng. Mater. Struct.*, 31 (2008) 714-724.
[33] D. Wang, W. Xiang and H. Zhu, Damage identification in beam type structures based on statistical moment using a two step method, *J. Sound Vib.*, 333 (3) (2014) 745-760.
[34] C. Liang, F. P. Sun and C. A. Rogers, Coupled electro-mechanical analysis of adaptive material systems-determination of the actuator power consumption and system energy transfer, *J. Intell. Mater. Syst. Struct.*, 8 (1997) 335-343.
[35] O. Bilgen, Y. Wang and D. J. Inman, Electromechanical comparison of cantilevered beams with multifunctional piezoceramic devices, *Mech. Syst. Signal Process.*, 27 (2012) 763-777.
[36] S. Zhou, Q. Chen and X. Wang, Convolutional deep networks for visual data classification, *Neural Process. Lett.*, 38 (1) (2013) 17-27.
[37] S. Mallat, *A Wavelet Tour of Signal Processing*, 2nd Edition, Academic Press, New York, USA (1999).

Osama Alazzawi was born in Iraq, 1987. He is a Ph.D. student of the School of Civil and Hydraulic Engineering, Huazhong University of Science and Technology, Wuhan, Hubei. He received his Master degree in Structural Engineering from SHUAST U.P, India. His research interests include structural health monitoring, structural dynamic and vibration control.
E-mail: alazzawi@hust.edu.cn; uraad@uowasit.edu.iq

Dansheng Wang is currently working as a Professor at School of Civil and Hydraulic Engineering, Huazhong University of Science and Technology Wuahn, China. He received his Ph.D. degree in Structural Engineering from Huazhong University of Science and Technology, China. His research includes the field of structural health monitoring, damage identification, smart material and structures and finite element method.
E-mail: danshwang@hust.edu.cn